Journal of Power Sources, 30 (1990) 209 - 226

THE AGGREGATE-OF-SPHERES ('KUGELHAUFEN') MODEL OF THE $PbO_2/PbSO_4$ ELECTRODE

A. WINSEL*, E. VOSS and U. HULLMEINE

VARTA Batterie AG, Research and Development Centre, D-6233 Kelkheim/Ts. (F.R.G.)

Introduction

In a recent publication, it was shown that the capacity of the $PbO_2/PbSO_4$ electrode is dependent upon the charge and discharge parameters. These particular phenomena have been related to the geometrical morphology of the porous $PbO_{2-\delta}$ active material.

The morphology of the active material can be regarded as a 'Kugelhaufen' or aggregate of spheres; a configuration similar to that of a sintered body. Therefore, it can be described by the mathematical model recently developed by Winsel *et al.* Since many of the well-known porous electrodes in practical battery systems exhibit this specific structure, it has been suggested that an experimental and theoretical treatment of a Kugelhaufen electrode would be of general significance.

Definition

An aggregate-of-spheres electrode is a porous body consisting of interconnected spherical particles. In such a body, it is possible to move from one inner point of a sphere to any second point in another sphere via a path that does not intersect the inner surface of the electrode body. Such bodies are generated by pressing and sintering pulverized materials or by electrochemical deposition.

Generation of an aggregate-of-spheres electrode

At the University of Kassel, the late H.-J. Euler [1] performed theoretical and experimental work for the better understanding of sinter processes. In his thesis, Metzendorf [2], one of Euler's students, correlated the limit of mass utilization to the interruption of the electronic paths. After the death of Euler, one of us (A. W.) continued his work and supplemented it by electrochemical experiments. This work, performed by Willer and Rückborn, has

*Author to whom correspondence should be addressed.

0378-7753/90/$3.50

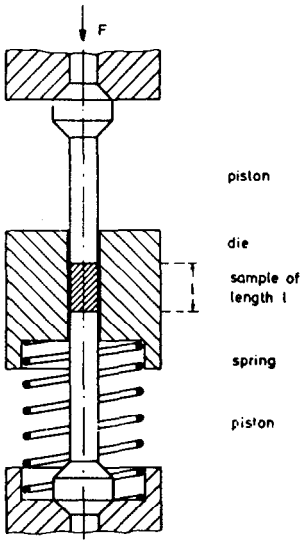

Fig. 1. Experimental device for measurement of conductivity of a pressed-powder specimen as a function of pressure.

recently been published [5]. The doctoral thesis of Willer [3] was related to the sinter behaviour of copper powder, whereas the diploma thesis of Rückborn [4] was directed towards the behaviour of cobalt powder. Figure 1 shows the experimental device for the measurement of the average specific conductivity of a pressed metal powder sample during compression. As shown in Fig.

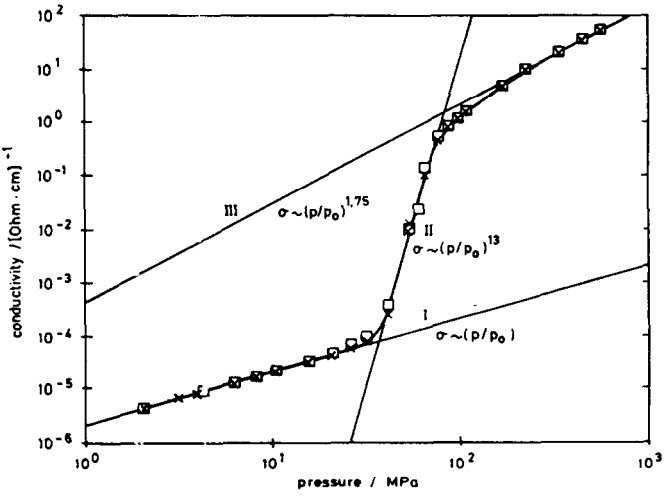

Fig. 2. Conductivity of compressed Co powder as a function of pressure. Region I: conductivity changes nearly proportional to pressure. Region II: very fast increase in conductivity due to metal bridges forming between powder particles. Region III: broadening of metal bridges.

2, three different regions can be distinguished for cobalt powder. At low pressure, the conductivity of the sample increases nearly proportionally to the applied pressure (region I). In region II, the conductivity increases very sharply and is proportional to about the 13th power of the pressure. This indicates the creation of an aggregate of spheres because the sharp increase in the conductivity is caused by the development of metal bridges between the original individual powder particles. On account of the high inner pressure, the oxide layers surrounding the individual particles are cracked by the creeping metal and thus cause cold welding throughout the sample. In region III, the metal bridges are broadened, as indicated by an increase in the conductivity of less than the second power of the pressure. The metallic bridges between the spherical-shaped particles expand for as long as the mechanical tension is greater than the yield strength of the material [5]. When the pressure is released, the samples remain highly conductive. From this, it follows that the metallic bridges are preserved and determine the conductivity.

In the experimental device shown in Fig. 3 [3], the conductivity and the dilatation of the samples are measured during increases in the temperature. Most of these experiments have been performed in an inert atmosphere or in air, others in a reducing atmosphere. Irrespective of the atmosphere, the following behaviour has been detected (see Fig. 4). At low temperatures, the specific resistance of a pressed cobalt powder sample increases with increasing temperature, as expected for a metal. A little above 200 °C, however, the resistance starts to decrease, although no change in the length of the sample (upper curve) occurs. At about 420 °C, there is a sharp decrease in the resistance and a small change in the length of the sample. This indicates a phase transition which is well known for cobalt. Up to about 600 °C, the resistance of the sample declines and eventually reaches its lowest value,

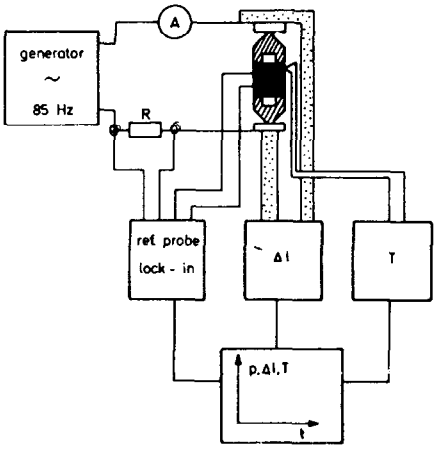

Fig. 3. Experimental arrangement for simultaneous measurements of conductivity and dilatation of pressed-powder samples as a function of temperature.

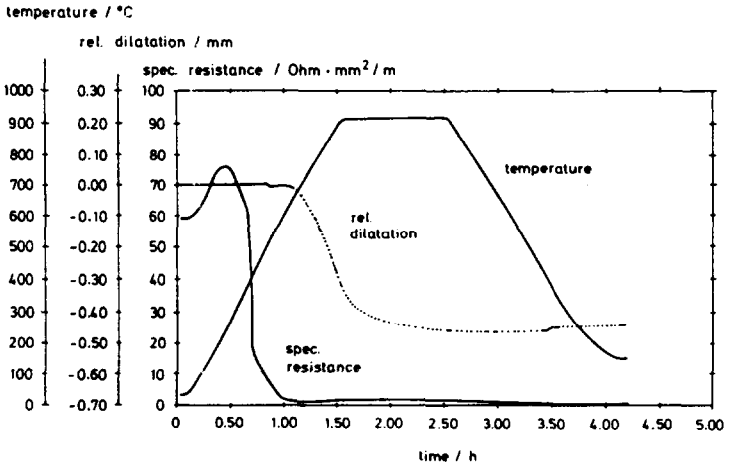

Fig. 4. Specific resistance and dilatation of a pressed cobalt powder specimen as a function of temperature.

accompanied by a shrinkage due to a material flow between the spheres. The same behaviour has been found for copper powder, as is shown in Fig. 5.

If the temperature is increased to 90 °C, the specific resistance behaves like a metallic conductor because it increases with increasing temperature and decreases with decreasing temperature. At temperatures above 90 °C, the resistance begins to fall. This is marked by point 1. If, at point 2, the temperature is decreased, then the resistance also decreases and the material behaves as a metal in the lower temperature region. If the temperature of the compressed body is raised above the highest value that has been previously reached, the resistance again begins to fall. This is shown at points 3 - 4. Until the resistance has reached its lowest value, no dilatation can be observed. After this, however, the shape change becomes very important, thus indicating creepage of the material. This creepage has also been demonstrated by microscopic observations [4].

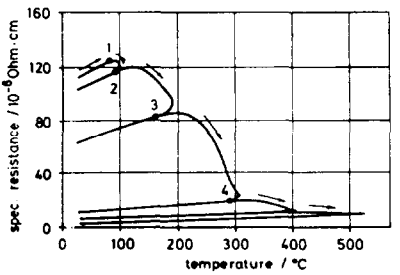

Fig. 5. Specific resistance of a pressed copper powder sample as a function of temperature. Numbers 1 to 4 indicate lines of decreasing and increasing temperature.

Geometry and Laplace pressure of an aggregate of spheres

The behaviour of the compressed metallic powder in which the individual spherical-shaped granules are connected by metallic necks can be understood as a material creepage in the neck region under the action of the surface tension. Figure 6 shows a simplified model of two spheres and the neck between them [5]. It must be remembered that the mean radii of the surface curvature of a sphere are both directed to the center of the sphere. The surface tension, σ, thus creates a Laplace pressure, p_k, according to eqn. (1):

$$p_k = \sigma(1/R + 1/R) = 2\sigma/R \tag{1}$$

In the neck region, the Laplace pressure, p_h, is determined by the neck radius, h, and the radius, r, of the groove, according to eqn. (2):

$$p_h = \sigma(1/h - 1/r) \tag{2}$$

The center of r is outside the material, thus contributing the negative term in eqn. (2) to the Laplace pressure, p_h, in the neck zone. A simple geometric calculation shows r to be a function of h according to eqn. (3):

$$r = h^2/2(R - h) \tag{3}$$

The Laplace pressure induced by the surface tension in the neck region has the tendency to broaden it by a mechanical stress as long as the stress tension is larger than the stress yield. If the temperature is increased, the softening process will result in a lower stress yield. Therefore, the neck radius, h, increases according to the flow of material from the adjacent spheres into the neck region. If an equilibrium is assumed between the pressure, p_h, and the yield strength, ε_o, [5], eqn. (4) can be derived by combining eqns. (1) - (3):

$$p_h = -2R\sigma[1 - 3h/2R]/h^2 = \varepsilon_o(T) \tag{4}$$

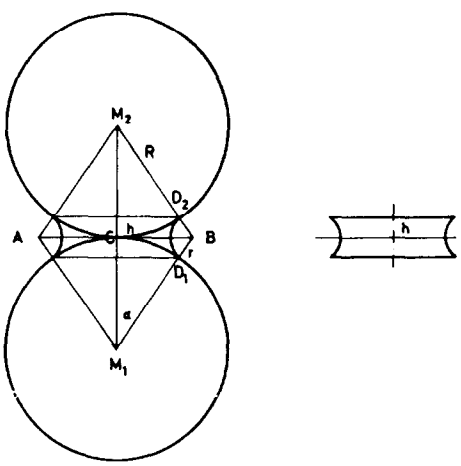

Fig. 6. Simplified model of two spheres and the neck between.

$\varepsilon_o(T)$ is a function of the temperature T and decreases with increasing temperature. Therefore, the neck radius h increases with increasing temperature. If $h \ll R$, eqn. (4) reduces to:

$$2R/h^2 = \varepsilon_o(T)/\sigma(T) \tag{5}$$

Specific resistance of an aggregate of spheres

A unit volume of an aggregate of spheres may contain n^3 particles of uniform radius, R. The volume, V_K, of each sphere is given by

$$V_K = 4\pi R^3/3 \tag{6}$$

For a porosity, P:

$$n^3 V_K = 1 - P \tag{7}$$

Substituting eqn. (6) in eqn. (7) gives:

$$n = [3(1 - P)/4\pi]^{1/3}/R \tag{8}$$

In an aggregate there may be n^2 conducting rows of spheres in parallel per unit volume, each line having n spheres in series and, subsequently, n necks on both sides, at which the neck resistance, w_H, is observed. The resistance of one single line, w_L, is given by:

$$w_L = 2nw_H \tag{9}$$

and, consequently, the specific resistance of the total aggregate, Ω, is:

$$\Omega = 2nw_H/n^2 = 2w_H/n \tag{10}$$

The neck resistance, w_H, at a narrow passage of radius h between two spheres of specific resistance, Ω°, is given by [3, 6]:

$$w_H = \Omega^\circ/4h \tag{11}$$

Using this expression in combination with eqns. (8) and (10) yields:

$$\Omega = \Omega^\circ(R/h)[\pi(1 - P)/6]^{1/3} \tag{12}$$

The term $[\pi(1 - P)/6]^{1/3}$ is close to unity. The product of this term together with the specific resistance of the bulk material, Ω°, describes the specific resistance, Ω^*, of an aggregate of the same geometry, but without narrow zones between the spheres. Therefore, changes in the electronic resistance that are due to changes in the neck geometry can be described by:

$$\Omega = \Omega^* R/h \tag{13}$$

Equation (5) describes the neck radius in equilibrium with the surface tension, σ, and the yield strength, ε_o, as a function of the temperature, T. By combining eqns. (5) and (13) it follows:

$$\Omega = \Omega^*(R\varepsilon_o/2\sigma)^{1/2} \tag{14}$$

In this equation, the parameter

$$\Gamma = 2\sigma/\varepsilon_o; \qquad [\Gamma] = \text{cm} \tag{15}$$

can be regarded as a specific length that describes the equilibrium of surface tension and inner stress in the neck region. Its value depends on the temperature and on other parameters that determine the surface tension (interfacial tension), *e.g.*, nature and concentration of the electrolyte, potential of the electrochemical double layer, etc.

Thermodynamics of an aggregate of spheres

If an electrochemical discharge reaction attacks the surface of an electrode evenly, the necks that are closest to the grid will disappear very soon after switching on the current. Therefore, it is an essential requirement that the neck zones of aggregate-of-spheres electrodes have potentials that protect them from being electrochemically sliced off on discharge. In metal electrodes, therefore, the neck potential is more noble, *e.g.*, more positive, than that of the sphere region. This describes the tendency of the neck to expand as if a lower metal vapour pressure exists to catch metal atoms. From this, it is expected that the neck region is a region of preferred 'underpotential deposition' (upd) of metal ions. In the case of oxides such as PbO_2, the potential of the neck region is more negative than that of the spheres. This negative potential again protects the neck from being electrochemically sliced off during passage of a discharge current.

In order to describe the above behaviour in thermodynamic terms, a constant molar volume, V_0, is assumed for the material in both the neck region and the sphere region. The chemical potential difference between these phases is:

$$\delta\mu = V_0(p_h - p_K) \tag{16}$$

Substituting eqns. (1) - (3) in eqn. (16) yields:

$$\delta\mu = (2V_0\sigma/R)[1 + (R^2/h^2) - (3R/2h)] \tag{17}$$

and, consequently, the potential difference, $\delta\Phi$, is given by:

$$\delta\Phi = -\delta\mu/zF = -(V_0\sigma/FR)[1 + (R^2/h^2) - (3R/2h)] \tag{18}$$

$$\approx -(V_0\sigma/FR)[1 + (R^2/h^2)] \tag{18a}$$

For $h \ll R$, the third term in the brackets of eqn. (18) can be neglected against the second one. Therefore, according to eqn. (18a) the potential in the neck zone deviates, by the second power of the R/h ratio, from the potential of the sphere.

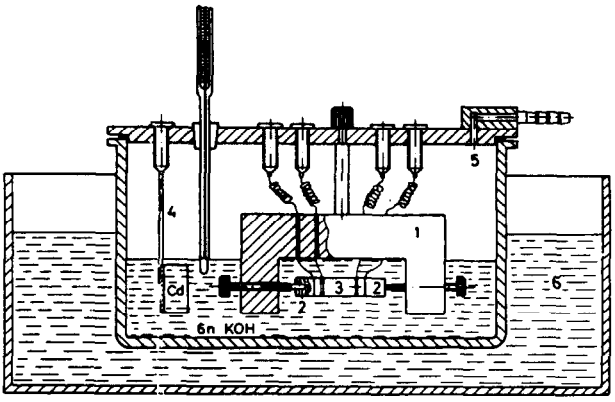

Fig. 7. Electrochemical cell for measurement of ohmic resistance of pressed powder specimens.

Electrochemical measurements on pressed-powder samples

Figure 7 shows a test cell design for the determination of the electronic resistance of a pressed powder sample during an electrochemical treatment consisting of dipping in the electrolyte and electrochemical reduction. Such measurements have been performed with copper samples as well as with cobalt samples. The results can be described as follows: at the moment when a pressed-powder sample of cobalt is dipped in the KOH electrolyte, the

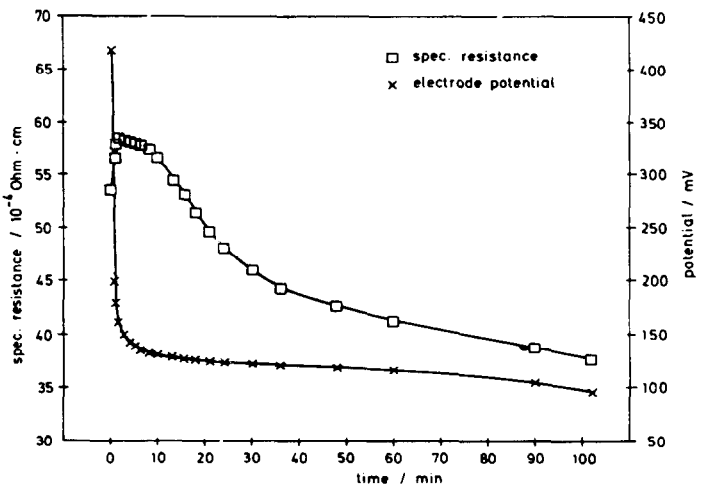

Fig. 8. Electronic resistance and potential of a pressed copper powder sample as function of time after soaking in KOH at room temperature.

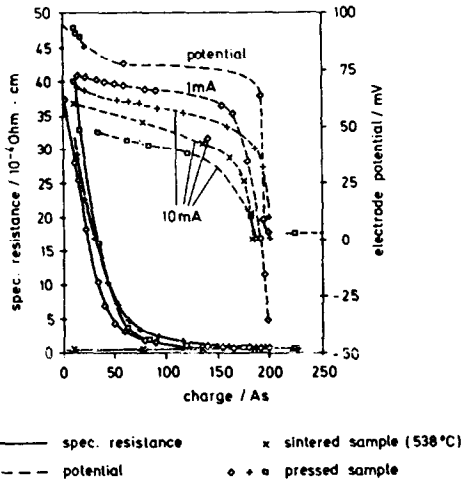

Fig. 9. Electronic resistance and potential of pressed copper powder samples during cathodic reduction as function of reduction charge.

potential against a $Cd/Cd(OH)_2$ reference electrode declines from very positive values by more than 250 mV during the first 10 min, as can be seen from Fig. 8. By contrast, the resistance increases by 10% in the very first minute, exhibits a maximum, and then decreases steadily to a value that corresponds to a heat treatment of about 400 °C. During cathodic reduction of the oxide layers, a further diminution of the resistance can be observed, comparable with a heat treatment at 530 °C, Fig. 9.

Pressed specimens of copper powder show a decrease in the sample resistance during cathodic reduction at the Cu_2O/Cu-potential, *e.g.*, from 112 to 7 $\mu\Omega$ cm.

These results can be interpreted by the aggregate-of-spheres model. As soon as the specimen is dipped in the alkaline solution, a wetting process takes place: water molecules are intercalated into the oxide layer, which swells. Simultaneously, the surface tension decreases due to the formation of the double layer. Both processes cause an increase in the neck resistance in the first minute. Under the influence of the potential difference, $\delta\Phi$, between the neck and the sphere, a local current is created by which copper ions originating from the dissolved CuO or Cu_2O layer are precipitated cathodically in the neck zone. This causes a broadening of the neck and a decrease in the resistance. As a result of this process, the potential difference, $\delta\Phi$, relaxes and brings the diminution of the resistance to an end. By implementation of an outer cathodic current to the sample, however, the reduction of the oxide layer is continued and causes a preferred deposition of copper ions in the neck region. This is the reason for the observed behaviour of the ohmic resistance of the aggregate of spheres.

PbO_2 electrode as an aggregate-of-spheres electrode

Battery engineers are aware that PbO_2 electrodes sometimes are only partly dischargeable, despite the fact that at the beginning of the experiment all of the active material consists of PbO_2. This feature has been observed in antimony-free electrodes [7] and has therefore been called the 'antimony-free effect' (AFE). There has been no real understanding of the AFE so far. One hypothesis claimed the growth of a lead sulphate layer as the reason for the AFE [8, 10].

Some years ago, it was stated [9] that the lead sulphate layer is not the reason, but the result, of the AFE and that the true cause can only be a changing current distribution from cycle to cycle. In this sense, the cause of the AFE was postulated as a changing conductivity of the cycled PbO_2 [9]. From eloflux experiments [12], it was possible to diagnose the AFE and to develop a therapy against it. It was shown that the AFE would be better named a 'relaxable insufficient mass utilization' (RIMU) because the phenomenon is independent of the absence or presence of antimony. With the aid of the aggregate-of-spheres model, it is possible to explain very easily the mechanism involved in the AFE in terms of a RIMU process [13].

Diagnosis and therapy of RIMU

The following observations have been made on the RIMU process.

(i) The cured, washed and dried PbO_2 electrode exhibits its highest capacity on the first discharge. On recharge, even by the very best regime, only about 90% of the initial capacity can be achieved in a second cycle.

(ii) The RIMU occurs when a deep-cycled PbO_2 electrode is discharged under high-rate and recharged under low-rate conditions. In particular, this is true if both processes are carried out with flow of electrolyte through the electrode pores and if a high overcharge factor is applied. Such treatment is called a 'bad cycling regime'.

(iii) The RIMU can be generated in less than 10 'bad cycles'.

(iv) By applying a bad cycle regime, the RIMU can also be obtained in electrodes containing antimony.

(v) The RIMU can be avoided by applying a 'good cycling regime' consisting of a high-rate recharge, without flow-through of electrolyte, in the first step, and a low-charge/low-overcharge step at the end of the recharging process.

(vi) An electrode that shows the RIMU regains its full capacity by being washed and dried after recharge. This capacity is the same as that in the very first discharge after curing.

(vii) An electrode that shows the RIMU partially regains its capacity if it is kept unused within the cell electrolyte for a long period.

(viii) An electrode that shows the RIMU (at least partially) regains its capacity by being heated in the electrolyte, or by being dipped into an antimony-containing sulphuric acid solution for 24 h.

From these findings, a plausible hypothesis has been derived that the RIMU is caused by an increasing electronic resistance within the active material. This resistance is located in the narrow neck zones of the aggregate of spheres and changes the current distribution in the active material. This results in an interrruption of the electronic paths in the PbO_2 near to the grid and thus renders more and more active material undischargeable.

The different treatments that allow the capacity to be re-established are effective due to the broadening of the neck zones. Therefore, under RIMU conditions, the electrode contains necks that are frozen in too small and too stressed states. The retrieval of the original capacity is due to the relaxation of the necks into a stress-free state.

Experimental evidence of the aggregate-of-spheres hypothesis

In order to confirm the aggregate-of-spheres hypothesis, measurements have been performed of the electronic resistance of the active PbO_2 material during cycling. Figure 10 shows a grid with platinum wires that serve as potential probes. The Faure-type electrode was cycled in an eloflux cell.

During discharge of the electrode, the potential (Fig. 11(a)) and the electronic resistance of the active material (Fig. 11(b)) remain approximately constant. This demonstrates that the consumption of active material by the discharge process has very little influence on the paths of the electrons, because the neck regions that mainly determine the resistance remain unaffected. Only at the end of discharge does the electronic resistance within the active mass, and more particularly between the grid and the active mass, increase in the typical way. This clearly shows that the necks are protected against discharge until the surfaces of the spheres become passivated with lead sulphate. At this stage, the local overvoltage no longer protects the necks from attack by the discharge current.

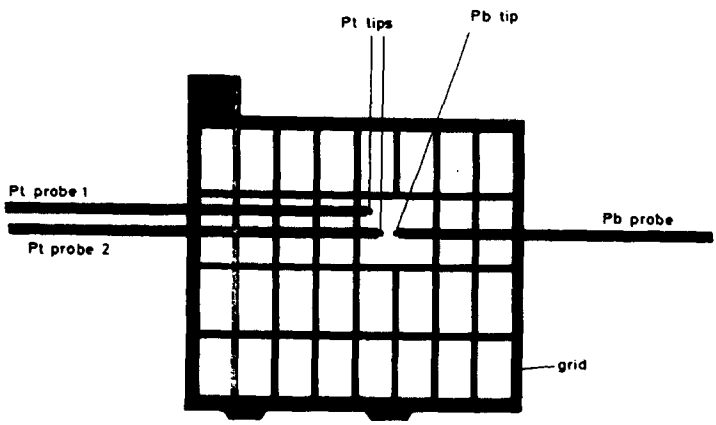

Fig. 10. Lead grid and the potential probes.

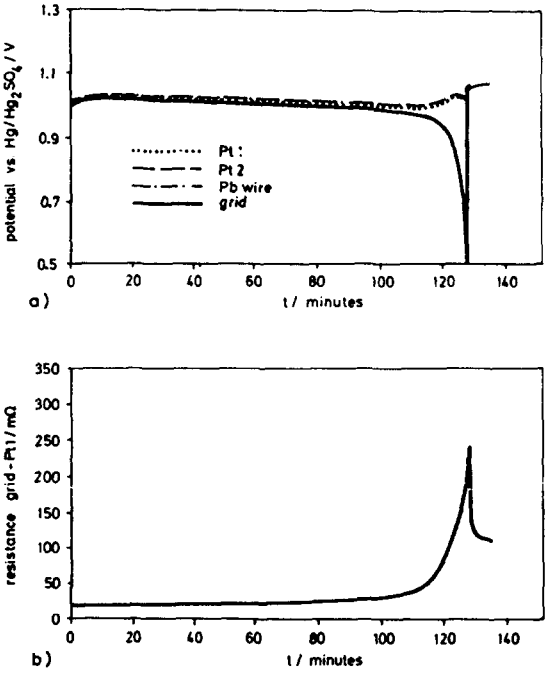

Fig. 11. (a) Potential, (b) electronic resistance of a PbO_2 electrode during discharge.

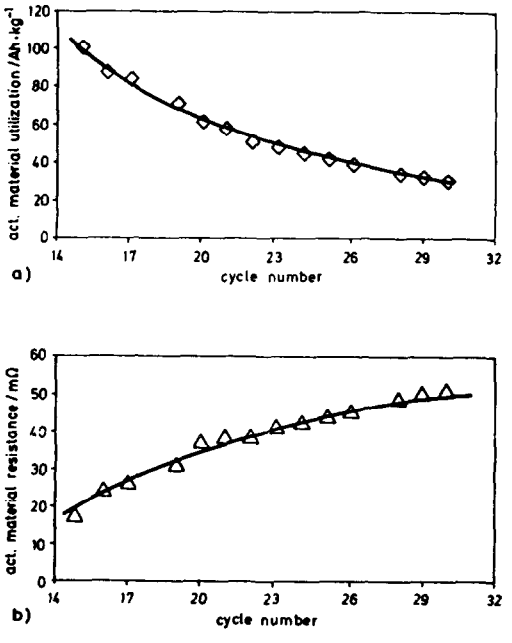

Fig. 12. (a) Material utilization, (b) electronic resistance of active material of a Faure PbO_2 electrode as a function of cycle number [11].

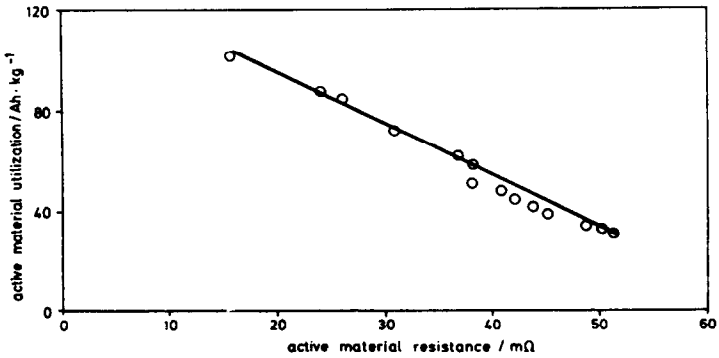

Fig. 13. Correlation between active mass utilisation and electronic resistance of active PbO_2.

Both the capacity and the resistance remain stable during cycling if a good cycle regime is applied to the electrode. If the electrode is exposed to a bad cycle regime, however, the conductance of the active material decreases simultaneously with the mass utilization. This behaviour is shown in Fig. 12 where curve (a) represents the material utilization and curve (b) depicts the material resistance as a function of the cycle number. Finally, Fig. 13 demonstrates the correlation between the active-mass utilization and the electronic resistance of the active material of the PbO_2 electrode. Treatments that help to recover a good utilization of material also simultaneously decrease the ohmic resistance of the active material [11].

Calculations on the PbO_2 aggregate-of-spheres electrode

Few fundamental data are known that allow the developed theory to be applied to the lead dioxide electrode. New information may be obtained, however, from the following calculations.

Thermodynamics, nucleation, growth and shedding

Spheres and necks in an aggregate-of-spheres electrode define two different phases of the same material that are in electrochemical equilibrium. Lead dioxide exhibits a certain composition range, $PbO_{2-\delta}$, that deviates from the stoichiometric composition by a deficiency, δ, of oxygen [13, 14]. This enables the system to balance the thermodynamic term $\delta\mu$ in eqn. (16) by a different stoichiometric deviation between the spheres, δ_R, and the necks, δ_h, with $\delta_h > \delta_R$. Since δ has an upper limit, $\delta\mu$ must equally have an upper limit, and therefore the quotient R/h according to eqn. (17) must also be limited. From this, it follows that during the formation of PbO_2 by electrochemical deposition, a two-dimensional nucleus must be formed to allow a new sphere to grow, from an existing one, into the surrounding solution. This two-dimensional nucleus should have the composition of the oxygen-poor PbO_2-phase, *i.e.*, of the crystallographic α-phase.

The composition range of lead dioxide is reported by Pohl and Rickert [14] to be:

$$0.003 < \delta < 0.016 \tag{19}$$

These authors describe the potential, Φ, of the PbO_2 electrode as a function of the stoichiometric deviation, δ, by the following relation:

$$\Phi = 0.991 - 0.124 \times \log \delta - 0.0592 \times \mathrm{pH} \tag{20}$$

This determines the potential difference, $\delta\Phi$, between the sphere and neck phases:

$$\delta\Phi = -0.124 \log(\delta_h / \delta_R) \tag{21}$$

Combining eqn. (21) with eqn. (18a) yields:

$$\log(\delta_h / \delta_R) = (8.04 V_0 \sigma / RF)(1 + R^2/h^2) \tag{22}$$

Although some of the parameters involved in eqn. (22) are unknown for lead dioxide, some important consequences can still be derived. If an anodic current is forced upon a fully charged $PbO_{2-\delta}$ electrode, the potential deviates to more positive values and brings (according to eqn. (21)) the stoichiometric deviation of the sphere phase, δ_R, to a minimum value. Therefore, the PbO_2 decomposes to its stable value, δ_{min}, and oxygen gas is evolved. Simultaneously, lead ions are sucked up by the sphere from the neck region because the surrounding solution is completely depleted of such ions. In order to remain within the composition range, the neck shrinks and, at least, reaches the minimal radius, h_{min}, and a maximum disorder, δ_{max}. The neck then vanishes leaving behind two individual spheres. It is proposed that this is the mechanism that gives rise to the shedding of the PbO_2 electrode because sliced-off particles with a closed surface have no tendency to grow together again. It follows, therefore, that high positive potentials at the charged electrode should be avoided since the potential induces shedding and the evolved oxygen transports the sludge out of the pores.

Minimum neck radius and maximum resistance

In order to evaluate eqn. (22), it would be necessary to know the δ_R value for $R \to \infty$. In addition, the surface tension, σ, is unknown. Nevertheless, it is useful to estimate the significance of eqn. (22). Therefore in addition to:

$$V_0 = 24.6\ \mathrm{cm^3\ mol^{-1}}; \qquad F = 96\,500\ \mathrm{C\ mol^{-1}}$$

the following values are assumed:

$$R = 10^{-5}\ \mathrm{cm}; \qquad \sigma = 10^{-4}\ \mathrm{J\ cm^{-2}}$$

The estimated radius, R, agrees with scanning electron microscopic and BET measurements. The value of the surface (interfacial) tension, σ, has been selected in accordance with data reported for solids [15, 16] that are correct in their order of magnitude. With such values for the various parameters, the

factor in eqn. (22) becomes:

$$(8.04 V_0 \sigma / RT) = 0.0205 \text{ V} \tag{23}$$

The quotient δ_h / δ_R can be estimated from the extreme values of eqn. (19). This gives:

$$\log(\delta_h / \delta_R) \leqslant \log(\delta_{max} / \delta_{min}) = \log(1.6 \times 10^{-2} / 3 \times 10^{-3}) = \log 5.33 = 0.727 \tag{24}$$

Equation (22) reduces by insertion of eqns. (23) and (24) to:

$$0.727 = 0.0205(1 + R^2/h^2) \tag{25}$$

and

$$R/h \leqslant 5.9 \tag{26}$$

Since the sphere radius has already been taken as $R = 10^{-5}$ cm, the neck radius can be calculated as $h = 0.17 \times 10^{-5}$ cm. This result is applied to the specific resistance of the aggregate-of-spheres electrode. From eqn. (13) it follows:

$$\Omega / \Omega^* \leqslant 5.9 \tag{27}$$

This relation suggests that values of the specific electronic resistance for a PbO_2 electrode, exposed to a bad and a good charging regime, vary in maximum by a factor of six.

The restorative process that leads to the original capacity by washing and drying of an electrode that exhibits the RIMU can be explained by a broadening of the necks corresponding to eqn. (14). When the electrode is kept in the electrolyte for a long period, the broadening proceeds via a very slow creepage of the material near the neck under the influence of the internal stress applied by the interfacial tension, σ. Heating of the electrode in the electrolyte assists this creepage by weakening the structure; the yield strength, ε_o, decreases with increasing temperature. The complete restoration of the initial capacity by washing and drying of the electrode makes use of an increased interfacial tension, σ. This is due to the omission of the electrochemical double layer which, if present, would have reduced the surface energy of the solid electrode.

Influence of charging regime on the RIMU

The aggregate-of-spheres model provides a key to understanding the influence of the charging regime on the capacity of the PbO_2 electrode during cycling. In particular, the question arises why a certain charge regime is a 'good regime' while another one turns out to be a 'bad regime'. In terms of the model, this reduces to the question: is it possible to understand how the charging regime influences the ratio R/h in eqn. (13) by referring to the parameters in eqn. (14)? The following is a possible answer.

During formation or recharge a spherical PbO_2 particle is created. The structure is determined by the local parameters σ and ε_o according to eqn. (14). σ is the interfacial tension of PbO_2 against sulphuric acid and depends

on the electrolyte concentration, the temperature, and the potential of the electrochemical double layer. The maximum interfacial tension in 4 M H_2SO_4 occurs close to 1.7 V *versus* SHE. Since the formation of PbO_2 takes place near the maximum of the interfacial tension and since σ exhibits little change in this region, it cannot be expected that there will be a potential influence on the structure via this parameter, σ.

The yield strength ε_o depends on the local temperature. The larger the specific current, the higher the overvoltage and the larger the energy dissipation. This results in a high local temperature and therefore in a decrease in the strength of the PbO_2.

The radius of the spheres, R, is a kinetically-determined parameter. As a result of the solution/precipitation mechanism, the lead ions must diffuse from the dissolving lead sulphate crystals to the growing lead dioxide spheres. It can be assumed that the radii of the spheres will become larger when the current per unit volume of active material is decreased. Indeed, if the current density is very high, the PbO_2 has the tendency to offer a very large and tree-like framework of well-conducting material to the migrating lead ions. This, together with the lower strength due to a higher local temperature, gives rise to a PbO_2 structure with a more favorable R/h ratio.

Conclusions

The model of the aggregate-of-spheres electrode describes the behaviour of the PbO_2 electrode under cycling conditions in a phenomenological way. It identifies the so-called 'antimony-free effect' (AFE) of the PbO_2 electrode as a 'relaxable insufficient mass utilization' (RIMU). In the case of a bad cycling regime, the RIMU is produced by the formation of smaller neck zones with increased restriction resistances. The increased specific resistance of the active material causes a change in the current distribution and, as a consequence, growing parts of the active material become isolated from the electronic conduction paths.

The model predicts the immunity of the neck zones against discharge, as well as the preferred underpotential deposition of ions in the neck region. On the basis of the limited composition range of $PbO_{2-\delta}$, the model also predicts that a two-dimensional nucleation is necessary for a new sphere to grow from an existing one during recharge. It is proposed that these neck zones exhibit the stoichiometric deviation of the α-PbO_2. In a fully charged electrode, an applied positive potential (overcharge) strangles the neck zones until the necks vanish and leave separated spheres behind. These separated PbO_2 particles form a sludge that can be washed out of the electrode pores by evolving oxygen gas, thus giving rise to the problem of plate shedding.

In summary, the Kugelhaufen model states or explains the following:

- the existence of two different phases, *e.g.*, the neck phase and the sphere phase, caused by different Laplace pressures of the surface curvature;

- the decreased apparent conductivity, compared with that of the bulk material, is determined by the constriction resistance of the necks;
- the increase of the apparent conductivity with increasing temperature is caused by softening of the material and broadening of the neck zones;
- the increase of the apparent conductivity after dipping the sample in an electrolyte solution is caused by cathodic deposition of metal and broadening of the neck zones as part of a local element action;
- the increase of the apparent conductivity by cathodic reduction is due to a preferred metal deposition in the neck zones;
- the protection against corrosion and discharge of the neck zones is caused by the thermodynamic potential difference of the phases;
- the preferred underpotential deposition (upd) in the neck zones is caused by a thermodynamic potential difference;
- the insufficient mass utilization of the PbO_2 electrode during cycling is caused by a decrease in the apparent conductivity, due to smaller necks;
- the relaxation of the insufficient mass utilization results from a broadening of the necks;
- a maximum and a minimum of the apparent conductivity, that differ by a factor of six, are due to the limited composition range of the $PbO_{2-\delta}$;
- the existence of a lower limit of the necks' radii is due to the presence of a maximum stoichiometric deviation;
- the growth of a new sphere from an existing one requires a two-dimensional nucleation in the neck region during recharge;
- any overpotential strangles the necks and causes shedding by sucking off lead ions from the neck zones and thus de-stabilizing the structure;
- the ratio of the necks' and spheres' radii depend upon the cycling regime on account of kinetic reasons; consequently, 'good' and 'bad' cycling regimes exist.

References

1 H.-J. Euler, *Metall, 35* (1981) 292 - 299.
2 H. Metzendorf, Elektronenleitfähigkeit der aktiven Massen von Bleiakkumulatoren während der Entladung und im Dauerbetrieb, *Dissertation*, Gesamthochschule Kassel, 1980.
3 B. Willer, Elektrische Leitfähigkeit und Dilatation bei Sintervorgängen, *Dissertation*, Gesamthochschule Kassel, 1984.
4 V.-E. Rückborn, Untersuchung der Sintervorgänge an Preßlingen aus Kobaltpulver, *Diplomarbeit*, Gesamthochschule Kassel, 1985.
5 V.-E. Rückborn, B. Willer and A. Winsel, *DECHEMA Monographien, Vol. 102*, VCH Verlagsgesellschaft, Weinheim, 1986, pp. 513 - 541.
6 R. Holm, *Electric Contacts*, Springer, Berlin, Heidelberg, New York, 1967.
7 J. Burbanks, A. C. Simon and E. Willihnganz, in P. Delahay and C. W. Tobias (eds.), *Adv. Electrochem. Eng., 8* (1971) 175.
8 S. Tudor, A. Weisstuch and S. H. Davang, *Electrochem. Technol., 3* (1965) 90; *4* (1966) 406; *5* (1967) 21.
9 U. Hullmeine, H. Laig-Hörstebrock, E. Voss and A. Winsel, Entwicklung einer Bleibatterie mit hoher Energie- und Leistungsdichte, Zuwendungsvertrag BMFT-ET 4046 A (1978).

10 D. Pavlov, The lead–acid cell, in B. D. McNicol and D. A. J. Rand (eds.), *Power Sources for Electric Vehicles*, Elsevier, Amsterdam, 1984.
11 W. Borger, U. Hullmeine, H. Laig-Hörstebrock and E. Meissner, *16th Int. Power Sources Symp., Bournemouth, 1988.*
12 J. Bohmann, U. Hullmeine, E. Voss and A. Winsel, Active material structure related to cycle life and capacity, *ILZRO Project LE-277, Final Rep., Dec. 1982.*
13 U. Hullmeine, E. Voss and A. Winsel, *J. Power Sources, 25* (1989) 27 - 47.
14 J. P. Pohl and H. Rickert, Electrochemistry of lead dioxide, in S. Trasatti (ed.), *Electrodes of Conductive Metallic Oxides*, Elsevier, Amsterdam, 1980.
15 *Handbook of Chemistry and Physics*, CRC-Press, Cleveland, 56th edn., 1975.
16 L. Mandelcorn, *Non-Stoichiometric Compounds*, Academic Press, New York, 1964.